

Improvement in Structural and Magnetic Properties of Electrospun $\text{Ni}_{1-x}\text{Cu}_x\text{Fe}_2\text{O}_4$ Nanofibers

Weiwei Pan^{1*}, Xinlei Zhang², Qin-Fang Liu², Jianbo Wang²

¹School of Physics and Electronic Science, Guizhou Normal College, Guiyang, China

²Institute of Applied Magnetism, Key Laboratory of Magnetism and Magnetic Materials of Ministry of Education, Lanzhou University, Lanzhou, China

Email: *panweiwei27@163.com

How to cite this paper: Pan, W.W., Zhang, X.L., Liu, Q.-F. and Wang, J.B. (2017) Improvement in Structural and Magnetic Properties of Electrospun $\text{Ni}_{1-x}\text{Cu}_x\text{Fe}_2\text{O}_4$ Nanofibers. *Soft Nanoscience Letters*, 7, 17-26.

<https://doi.org/10.4236/sn.2017.72002>

Received: September 19, 2017

Accepted: November 6, 2017

Published: November 9, 2017

Copyright © 2017 by authors and Scientific Research Publishing Inc.

This work is licensed under the Creative Commons Attribution International License (CC BY 4.0).

<http://creativecommons.org/licenses/by/4.0/>



Open Access

Abstract

A series of $\text{Ni}_{1-x}\text{Cu}_x\text{Fe}_2\text{O}_4$ ($0.0 \leq x \leq 1.0$) nanofibers have been synthesized employing electrospinning method at 650°C . The effect of Cu substitution on structural, morphology and magnetic properties of NiFe_2O_4 nanofibers is reported. The XRD analysis showed the formation of single-phase cubic spinel Ni-Cu ferrite and an increasing behavior of lattice constant. The surface morphology is characterized by SEM, it is investigated that nanofibers have uniform and continuous morphology. The VSM results showed Cu substitution played an important role in magnetic properties of $\text{Ni}_{1-x}\text{Cu}_x\text{Fe}_2\text{O}_4$. The saturation magnetization (M_s) decreases linearly with increasing Cu^{2+} content, while coercivity (H_c) has slowly decreased before $x \leq 0.5$, and then sharply increased to 723.9 Oe for $x = 1.0$. The magnetic properties of $\text{Ni}_{1-x}\text{Cu}_x\text{Fe}_2\text{O}_4$ can be explained in Neel's model, cation distribution and shape anisotropy.

Keywords

NiCu Ferrite, Electrospinning, Magnetic Properties, Nanostructures

1. Introduction

One-dimensional (1D) nanostructures of spinel ferrite have been a subject of intense research for their interesting chemical and physical properties which different from those of bulk materials [1]. Spinel ferrite with a general formulae MFe_2O_4 (where $\text{M} = \text{Co}, \text{Ni}, \text{Fe}, \text{Mg}, \text{Mn}, \text{Zn}, \text{and Cu}$) are widely used for many kinds of industrial applications such as optical, catalytic, sustainable hydrogen production application and electronic and magnetic devices [2] [3] [4]. Among,

NiFe_2O_4 is a one of most investigated spinel ferrite because of their remarkable properties such as high electrical resistivity, high mechanical hardness, large permeability at high frequency and chemical stability. The structural and magnetic properties of NiFe_2O_4 are particularly affected at cation distribution and the type of substitution [5] [6]. Among many ion doping, Cu substitution NiFe_2O_4 have been the subject of extensive investigation because of the high frequency application as magnetic materials [7]. NiFe_2O_4 is a completely inverse spinel ($\text{Fe}[\text{NiFe}]_2\text{O}_4$), Ni^{2+} have a strong preference for octahedral site (B-site), while CuFe_2O_4 is a partial inverse spinel ($\text{Cu}_x\text{Fe}_{1-x}[\text{Cu}_{1-x}\text{Fe}_{1+x}]\text{O}_4$), Cu^{2+} have a preference for tetrahedral site (A-site) and B-site. The substitution of Cu in NiFe_2O_4 brings about a structural phase transition, makes them a suitable material for various technological applications due to the interesting magnetic and electrical properties [8] [9].

In earlier work, with increasing copper content the saturation magnetization of $\text{Ni}_{1-x}\text{Cu}_x\text{Fe}_2\text{O}_4$ microparticles prepared by double-sintering method decreases linearly, whereas coercivity decreases up to $x = 0.6$ and then increases [10]. The effect of Cu substitution on chemical states of surface ions and surface composition in $\text{Ni}_{1-x}\text{Cu}_x\text{Fe}_2\text{O}_4$ spherical nanoparticles prepared by sol-gel combustion method [11], and the effect of Cu^{2+} substitution on electromagnetic properties of $\text{Ni}_{1-x}\text{Cu}_x\text{Fe}_2\text{O}_4$ nanoparticles is well studied [12]. Similar structure and magnetic properties are obtained for $\text{Ni}_{1-x}\text{Cu}_x\text{Fe}_2\text{O}_4$ nanostructures prepared by citrate-gel auto combustion technique [13], microwave-induced combustion [14], co-precipitation method [15] [16], and ceramic method [17] [18]. Compared to commercial mechanical process, electrospinning represents a simple, effective and convenient method for generating 1D nanofibers [19]. One of the most important advantages of electrospinning is the ability to control the component of composites, morphology and diameter of nanofibers. Electrospun nanofibers have been applied in a broad range of applications owing to their large specific surface area, high aspect ratio, and good dimensional stability [20].

In this paper, a series of $\text{Ni}_{1-x}\text{Cu}_x\text{Fe}_2\text{O}_4$ (where, $x = 0.0, 0.3, 0.5, 0.7, 1.0$) nanofibers have been prepared by electrospinning method. The effect of Cu substitution on structural, morphology and magnetic properties of NiFe_2O_4 nanofibers will be studied.

2. Experimental

2.1. Preparation of $\text{Ni}_{1-x}\text{Cu}_x\text{Fe}_2\text{O}_4$ Nanofibers

In this study, the raw materials including $\text{Ni}(\text{NO}_3)_2 \cdot 6\text{H}_2\text{O}$, $\text{Cu}(\text{NO}_3)_2 \cdot 3\text{H}_2\text{O}$, $\text{Fe}(\text{NO}_3)_3 \cdot 9\text{H}_2\text{O}$ and PVP (polyvinylpyrrolidone, $M_w \approx 1,300,000$) were of analytical grade and purchased from Tianjin Guangfu. DMF (*N,N*-Dimethylformamide, 99.7% purity, Tianjin Guangfu, China) and ethanol (100% purity) were used as solvents. In the solution preparation, 0.1 g of PVP was dissolved in mixture of ethanol and DMF with a weight ratio of 1:1, followed by magnetic stirring for 2 h to ensure the dissolution of PVP. Then $\text{Ni}(\text{NO}_3)_2 \cdot 6\text{H}_2\text{O}$,

$\text{Cu}(\text{NO}_3)_2 \cdot 3\text{H}_2\text{O}$, $\text{Fe}(\text{NO}_3)_3 \cdot 9\text{H}_2\text{O}$ with a molar ratio of $(1-x):x:2$ were added into the mixture solution. After having been stirred for 2 h, the homogeneous viscous solution was transferred into a plastic syringe in which a needle made of stainless steel was connected to a high-voltage equipment. The applied voltage was kept at +15 kV during the electrospinning process. The nanofibers were collected on a piece of aluminum foil about 15 cm below the tip of needle. All electrospinning processes were carried out at room temperature. The collected $\text{Ni}_{1-x}\text{Cu}_x\text{Fe}_2\text{O}_4/\text{PVP}$ precursor nanofibers were dried at 80°C for 3 h, and calcined at 650°C for 3 h in ambient atmosphere with a heating rate of $1^\circ\text{C}/\text{min}$.

2.2. Characterization

The calcined nanofibers were characterized by X-ray diffraction (XRD) pattern using $\text{CuK}\alpha$ radiation with $\lambda = 0.15418$ nm (PANalytical diffractometer). The scanning electron microscope (SEM, Hitachi S-4800) and transmission electron microscope (TEM, TecnaiTM G² F30, FEI) were employed to analyze morphology and microstructure of samples. Infrared spectra were obtained using Fourier transform infrared spectroscopy (FT-IR, Nicolet 6700) in the $400 - 4000$ cm^{-1} range. The magnetic properties of nanofibers were measured at room temperature using vibrating sample magnetometer (VSM, Lakeshore 7403, USA) with a maximum applied field of 12 kOe.

3. Results and Discussion

3.1. Structural Studies

The effect of Cu substitution on structural and morphology of NiFe_2O_4 nanofibers was been studied by XRD, SEM and TEM. The XRD patterns of synthesized $\text{Ni}_{1-x}\text{Cu}_x\text{Fe}_2\text{O}_4$ nanofibers calcined at 650°C for 3 h are shown in **Figure 1**. All of main diffraction peaks are indexed as the cubic spinel structure, no second phase can be detected. The position of peaks is slightly shifted to lower angle with increasing Cu^{2+} content. The diffraction peaks of samples for $x \leq 0.5$ correspond to

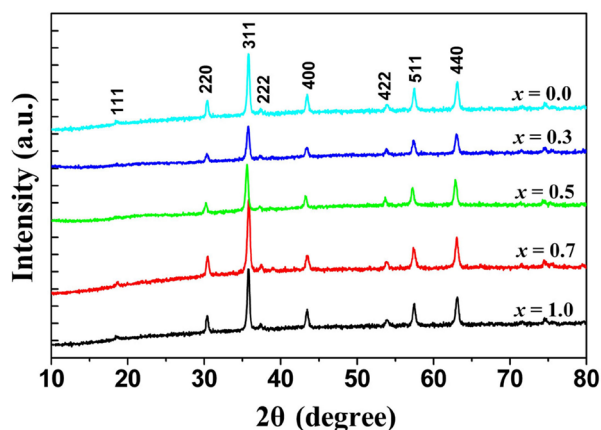


Figure 1. X-ray diffraction patterns of $\text{Ni}_{1-x}\text{Cu}_x\text{Fe}_2\text{O}_4$ ($0.0 \leq x \leq 1.0$) nanofibers calcined at 650°C for 3 h.

NiFe₂O₄, while the diffraction peaks of samples for $x \geq 0.7$ correspond to CuFe₂O₄. The lattice constant a is calculated by using equation:

$$a = d(h^2 + k^2 + l^2), \quad (1)$$

where d is the interplanar distance and h, k, l is the Miller indices of plane [21]. The average crystallite size D is calculated using Debye-Scherrer's formula with respect to peak plane (311). The values of a and D are extracted and listed in **Table 1**. From **Table 1** it can be seen that lattice constant increases with increasing Cu²⁺ content. The increased a may be explained on the bigger ionic radii of Cu²⁺ ions (0.72 Å) than Ni²⁺ ions (0.69 Å), indicating Cu²⁺ ions can be effectively built into NiFe₂O₄ lattice. The average crystallite size increases initially with Cu²⁺ contents, the maximum D occurs at $x = 0.5$ ($D = 24.1$ nm), and then decreases. The variation of a and D with Cu²⁺ content mainly attributed to the Cu²⁺ ions insert into the cubic spinel structure, the similar trends were observed in Ni_{1-x}Cu_xFe₂O₄ nanoparticles prepared by sol-gel combustion method [11].

3.2. Morphological Studies

The morphology of Ni_{1-x}Cu_xFe₂O₄ nanofibers were investigated by SEM and TEM. **Figure 2** shows the SEM images of Ni_{1-x}Cu_xFe₂O₄ nanofibers calcined at 650°C. It can be seen that all samples remained as continuous and randomly oriented morphology, the diameter of nanofibers is about 50 - 60 nm. The surface of nanofibers is smooth when x less than 0.3, rough surface were observed after x increasing to 0.5 and 0.7, the surface of CuFe₂O₄ nanofibers ($x = 1.0$) consists of small open porosity. A similar result was also observed in Ni_{0.5-x}Cu_xZn_{0.5}Fe₂O₄ nanofibers with $x = 0.0 - 0.5$ prepared by electrospinning [22]. The Cu²⁺ content has some influences on morphology of Ni_{1-x}Cu_xFe₂O₄ nanofibers. **Figure 3** shows the typical TEM (a-b) and HRTEM (c-d) images of Ni_{0.5}Cu_{0.5}Fe₂O₄ nanofibers, respectively. From **Figure 3(a)** and **Figure 3(b)**, it can be seen that these nanofibers exhibited a fibrous, continuous and good dispersity morphology, and a nanofiber is composed of randomly aligned nanoparticles. This is well consistent with that observed from SEM (**Figure 2**). In HRTEM image of Ni_{0.5}Cu_{0.5}Fe₂O₄ nanofibers (**Figure 3(c)**), the crystalline phase has well-resolved lattice fringes. The value of distance between the adjacent

Table 1. Parameters extracted from XRD and VSM for Ni_{1-x}Cu_xFe₂O₄ nanofibers system: lattice constant (a), average crystallite size (D), saturation magnetization (M_s), remanent magnetization (M_r) and coercivity (H_c).

Sample	Lattice constant a (Å)	Average Crystallite size D (nm)	M_s (emu/g)	M_r (emu/g)	H_c Oe
$x = 0.0$	8.3187	20.9	47.0	14.9	172.2
$x = 0.3$	8.3223	23.4	45.1	14.3	169.0
$x = 0.5$	8.3344	24.1	40.3	13.0	165.3
$x = 0.7$	8.3525	20.4	34.8	11.8	189.4
$x = 1.0$	8.3856	19.7	31.8	14.9	723.9

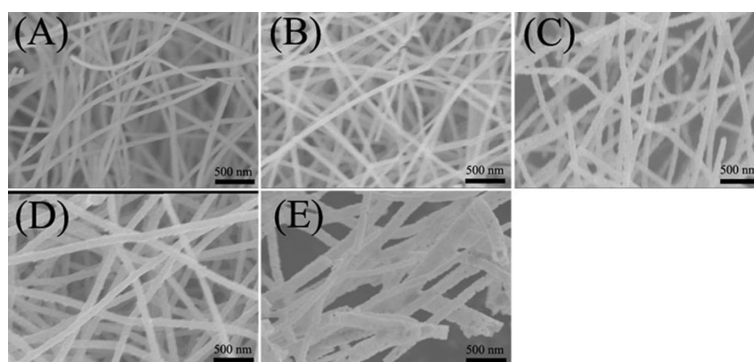


Figure 2. SEM images of $\text{Ni}_{1-x}\text{Cu}_x\text{Fe}_2\text{O}_4$ nanofibers with different Cu^{2+} content: (A) $x = 0.0$; (B) $x = 0.3$; (C) $x = 0.5$; (D) $x = 0.7$ and (E) $x = 1.0$.

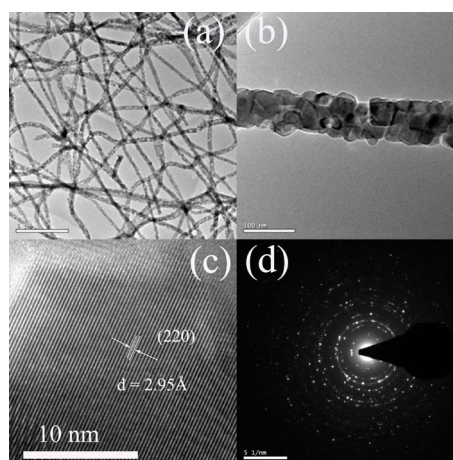


Figure 3. (a) (b) TEM images; (c) HRTEM image; and (d) SAED pattern of $\text{Ni}_{0.5}\text{Cu}_{0.5}\text{Fe}_2\text{O}_4$ nanofibers.

lattice is 2.95 \AA , which is in agreement with the XRD patterns. As shown in **Figure 3(d)**, selected area electron diffraction (SEAD) of $\text{Ni}_{0.5}\text{Cu}_{0.5}\text{Fe}_2\text{O}_4$ nanofibers consists of multiple intense rings, indicating that the sample has a polycrystalline nature.

3.3. FT-IR Studies

The ideal spinel structure consists of two sub-lattices, namely tetrahedral sites (A) and octahedral sites (B). Different charge combinations of metal cations are distributed in A and B sites. Therefore, the magnetic properties of spinel ferrite are to a large extent determined by the class of metal ions and cation distribution among the A and B sites. In $\text{Ni}_{1-x}\text{Cu}_x\text{Fe}_2\text{O}_4$ nanofibers, the replacement of Ni^{2+} ions with Cu^{2+} ions at B sites will influence the magnetic properties of samples. FT-IR spectra is usually assigned to the vibration of ions in crystal lattice, which can be used to confirm the positions of Ni^{2+} , Cu^{2+} , and Fe^{3+} ions in spinel structure. The vibrating sample magnetometer is used to measure the magnetic properties of samples.

Figure 4 shows the typical FT-IR spectra of $\text{Ni}_{1-x}\text{Cu}_x\text{Fe}_2\text{O}_4$ nanofibers recorded

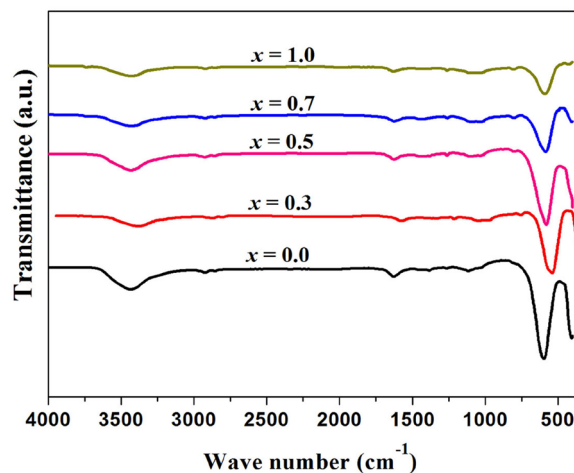


Figure 4. FT-IR spectra of $\text{Ni}_{1-x}\text{Cu}_x\text{Fe}_2\text{O}_4$ ($0.0 \leq x \leq 1.0$) nano-fibers.

between 4000 and 400 cm^{-1} . In the range of 1000 - 400 cm^{-1} , two main absorption bands of ferrite are appear. The absorption band $\nu_1 = 580 \text{ cm}^{-1}$ is assigned to the stretching vibration of tetrahedral complexes ($\text{Fe}^{3+}\text{-O}^{2-}$), and the absorption band $\nu_2 = 400 \text{ cm}^{-1}$ is attributed to the octahedral complexes ($\text{Fe}^{3+}\text{-O}^{2-}$). The peak intensity of ν_1 decreases with increasing Cu^{2+} contents, while the position band is shifted to lower frequencies. Synchronously, the intensity and position of ν_2 changed slightly with x . Similar results are observed in $\text{Ni}_{1-x}\text{Cu}_x\text{Fe}_2\text{O}_4$ nanoparticles prepared by sol-gel combustion method [11] [23]. The difference in band position of ν_1 and ν_2 can be related to the difference in $\text{Fe}^{3+}\text{-O}^{2-}$ bond lengths at A sites and B sites. It was found that the Fe-O distance at A sites (1.89 Å) is smaller than that of the B sites (2.03 Å) [24] [25]. When Ni^{2+} ions is replaced by Cu^{2+} ions, due to charge imbalance some Fe^{3+} ions shift from A sites to B sites, making the $\text{Fe}^{3+}\text{-O}^{2-}$ stretching vibration in greater. So the decrease in peak intensity of ν_1 with increasing Cu^{2+} content is mainly attributed to the change in $\text{Fe}^{3+}\text{-O}^{2-}$ bands.

3.4. Magnetic Studies

The magnetic structure of spinel ferrite is ferrimagnetic, the magnetic moments of A and B sites are coupled antiparallel to each other. There are twice as many B sites filled, so there is a net magnetic moment equal to the difference between the two sites. The magnetization behavior of spinel ferrite can be understood in Neel's model. In $\text{Ni}_{1-x}\text{Cu}_x\text{Fe}_2\text{O}_4$ nanofibers, the composition and cation distribution among the A and B sites will influence the magnetic properties of samples. **Figure 5** shows magnetic hysteresis loops for $\text{Ni}_{1-x}\text{Cu}_x\text{Fe}_2\text{O}_4$ nanofibers measured at room temperature, the values of saturation magnetization (M_s), remanent magnetization (M_r) and coercivity (H_c) are calculated from loops and given in **Table 1**. From the figure it is noticed that the value of M_s decreases linearly with increasing Cu^{2+} content, while M_r gradually decreases up to $x = 0.7$, then increases small for $x = 1.0$. The H_c decreases up to $x = 0.5$ with x , after it sharply

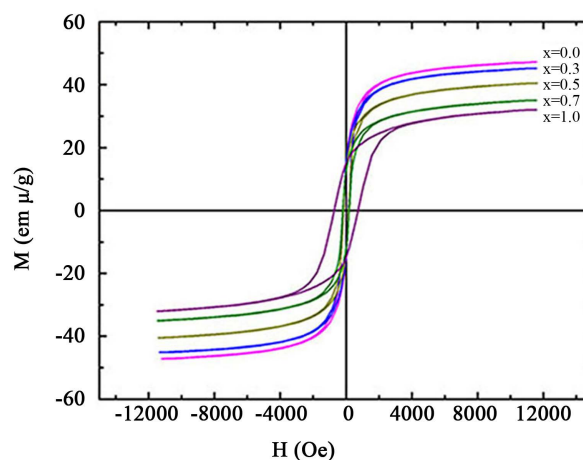


Figure 5. Magnetic hysteresis loops for $\text{Ni}_{1-x}\text{Cu}_x\text{Fe}_2\text{O}_4$ ($0.0 \leq x \leq 1.0$) nanofibers at room temperature.

increase to 723.9 Oe for $x = 1.0$.

According to Neel's model, the magnetic moment per formula is expressed as:

$$\mu_B = M_B(x) - M_A(x), \quad (2)$$

where M_B and M_A are magnetic moments of B and A sites in μ_B . It is well known NiFe_2O_4 is an inverse spinel structure, all Ni^{2+} ion and a Fe^{3+} ion occupy B sites, other Fe^{3+} ion occupy A sites. CuFe_2O_4 is a partial inverse spinel structure with 85% Cu^{2+} at B sites, other 15% at A sites [25]. The magnetic moment of Cu^{2+} ions ($1.0 \mu_B$) is smaller than Ni^{2+} ions ($2.3 \mu_B$) [23]. The Cu^{2+} ions are substituted instead of Ni^{2+} ions result in a decrease in net magnetic moment of samples. A part of Cu^{2+} ions occupy A sites leading to a migration of Fe^{3+} ions from A sites to B sites. With increasing Cu^{2+} content, the super-exchange interaction between A and B sites decreases. Therefore, the decrease trend in saturation magnetization and remanent magnetization is agreed with that of an expected decrease in $\text{Ni}_{1-x}\text{Cu}_x\text{Fe}_2\text{O}_4$ nanofibers.

The variation of H_c with Cu^{2+} contents can be understood on basis of domain structure, anisotropy and critical diameter [26]. The initial decrease trend of H_c ($x \leq 0.5$) is due to the increase in crystallite size, which is observed in XRD results. This may be attributed to the magnetization mechanism which is a domain rotation process. The H_c value of 723.9 Oe obtained for CuFe_2O_4 nanofibers in present work is higher than the value of 93.7 Oe and 151.0 Oe of CuFe_2O_4 nanoparticles prepared by double-sintering method and coprecipitation method, respectively [10] [23]. This value is also higher than $H_c = 625.0$ Oe for CuFe_2O_4 nanofibers prepared by electrospinning method [27]. The high value of H_c in this paper may be attributed to the magnetocrystalline and shape anisotropy. The magnetocrystalline anisotropy of CuFe_2O_4 nanofibers is about 0.6×10^5 erg cm^{-3} , while shape anisotropy is calculated to be $k_s = 1.7 \times 10^5$ erg cm^{-3} using the measured M_s (31.8 emu g^{-1}) [28], which is higher than magnetocrystalline anisotropy. Therefore, the high H_c of CuFe_2O_4 nanofibers mainly come from shape

anisotropy if we neglect the dipolar interactions between nanofibers. In Refer. 15, the breakdown of fibers morphology result to lower H_c than this work, while in this paper CuFe_2O_4 sample retain favorable nanofibers morphology.

4. Conclusion

The class of metal ions and cation distribution among A and B sites will affect the magnetic properties of spinel ferrite. Nanofibers morphology produced a difference characteristic compare with nanoparticles ones. In this paper, $\text{Ni}_{1-x}\text{Cu}_x\text{Fe}_2\text{O}_4$ nanofibers ($0.0 \leq x \leq 1.0$) were prepared by electrospinning method, the effect of copper substitution on structure, morphology and magnetic properties of NiFe_2O_4 nanofibers is studied. Increasing the Cu^{2+} ion causes an increase in lattice constant due to the larger ionic radii of Cu ion. All samples remain as continuous fibers morphology, while surface of nanofibers with $x \leq 0.3$ is smooth, it becomes rough and porous for $x = 0.5 - 0.7$ and $x = 1.0$. FT-IR spectra is used to confirmed the positions of Ni^{2+} , Cu^{2+} , and Fe^{3+} ions in spinel structure. Magnetic properties of $\text{Ni}_{1-x}\text{Cu}_x\text{Fe}_2\text{O}_4$ nanofibers are studied using vibrating sample magnetometer at room temperature. With increasing Cu^{2+} content, the saturation magnetization (M_s) was observed to decrease, while the coercivity (H_c) decreased up to $x = 0.5$ and then sharply increased to 723.9 Oe for $x = 1.0$. The high coercivity of CuFe_2O_4 nanofibers compare with nanoparticles samples mainly comes from shape anisotropy of nanofibers. These observations provided by this work gave a fundamental understanding of nanofibers morphology prepared by electrospinning method.

Acknowledgements

This paper was supported by the Science and Technology Fund of Guizhou (J[2014]2143), the Scientific Research Fund of Guizhou Normal College (13BS014) and the Grant of Guizhou Normal College (107003001455).

References

- [1] Sugimoto, M. (1999) The Past, Present, and Future of Ferrites. *Journal of the American Ceramic Society*, **82**, 269-280. <https://doi.org/10.1111/j.1551-2916.1999.tb20058.x>
- [2] Manikandan, A., Sridhar, R., Antony, S.A. and Ramakrishna S. (2014) A Simple Aloe Vera Plant-Extracted Microwave and Conventional Combustion Synthesis: Morphological, Optical, Magnetic and Catalytic Properties of CoFe_2O_4 Nanostructures. *Journal of Molecular Structure*, **1076**, 188-200. <https://doi.org/10.1016/j.molstruc.2014.07.054>
- [3] Valan, M.F., Manikandan, A. and Arul Antony, S. (2015) A Novel Synthesis and Characterization Studies of Magnetic Co_3O_4 Nanoparticles. *Journal of Nanoscience and Nanotechnology*, **15**, 4580-4586. <https://doi.org/10.1166/jnn.2015.9776>
- [4] Mathubala, G., Manikandan, A., Arul Antony, S. and Ramar, P. (2016) Photocatalytic Degradation of Methylene Blue Dye and Magneto-Optical Studies of Magnetically Recyclable Spinel $\text{Ni}_x\text{Mn}_{1-x}\text{Fe}_2\text{O}_4$ ($x = 0.0 - 1.0$) Nanoparticles. *Journal of Molecular Structure*, **1113**, 79-87. <https://doi.org/10.1016/j.molstruc.2016.02.032>

- [5] Gupta, N., Jain, P., Rana, R. and Shrivastava, S. (2017) Current Development in Synthesis and Characterization of Nickel Ferrite Nanoparticle. *Materialstoday: Proceeding*, **4**, 342-349. <https://doi.org/10.1016/j.matpr.2017.01.031>
- [6] Horvath, M.P. (2000) Microwave Applications of Soft Ferrites. *Journal of Magnetism and Magnetic Material*, **215-216**, 171-183. [https://doi.org/10.1016/S0304-8853\(00\)00106-2](https://doi.org/10.1016/S0304-8853(00)00106-2)
- [7] Zaki, H.M. (2012) Structure, Analysis and Some Magnetic Properties for Low Temperature Fired Ni-Cu Ferrite. *Physics B Condensed Matter*, **407**, 2025-2031. <https://doi.org/10.1016/j.physb.2012.01.134>
- [8] Rezlescu, N. and Rezlescu, E. (1974) Abnormal Dielectric Behaviour of Copper Containing Ferrites. *Solid State Communications*, **14**, 69-72. [https://doi.org/10.1016/0038-1098\(74\)90234-8](https://doi.org/10.1016/0038-1098(74)90234-8)
- [9] Dimri, M.C., Verma, A., Kashyap, S.C., Dube, D.C. and Thakur, O.P. (2006) Structural, Dielectric and Magnetic Properties of NiCuZn Ferrite Grown by Citrate Precursor Method. *Materials Science and Engineering: B*, **133**, 42-48. <https://doi.org/10.1016/j.mseb.2006.04.043>
- [10] Anjum, S., Rashid, A., Bashir, F., Pervaiz, M. and Zia, R. (2015) Effect of Cu Doped Nickel Ferrites on Structural, Magnetic and Dielectric Properties. *Materialstoday: Proceeding*, **2**, 5559-5567. <https://doi.org/10.1016/j.matpr.2015.11.086>
- [11] Tan, X.Y., Li, G.Y., Zhao, Y. and Hu, C.W. (2009) The Effect of Cu Content on the Structure of $Ni_{1-x}Cu_xFe_2O_4$ Spinel. *Materials Research Bulletin*, **44**, 2160-2168. <https://doi.org/10.1016/j.materresbull.2009.08.018>
- [12] Azadmanjiri, J., Salehani, H.K., Barati, M.R. and Farzan, F. (2007) Preparation and Electromagnetic Properties of $Ni_{1-x}Cu_xFe_2O_4$ Nanoparticle Ferrites by Sol-Gel Auto-Combustion Method. *Materials Letters*, **61**, 84-87. <https://doi.org/10.1016/j.matlet.2006.04.011>
- [13] Sridhar, R., Ravinder, D. and Vijaya Kumar, K. (2015) Temperature-Dependence Thermoelectric Power Studies of Mixed Ni-Cu Nano Ferrites. *Journal of Alloys and Compounds*, **645**, 436-442. <https://doi.org/10.1016/j.jallcom.2015.05.041>
- [14] Elshahawy, A.M., Mahmoud, M.H., Makhlof, S.A. and Hamdeh, H.H. (2015) Role of Cu^{2+} Substitution on the Structural and Magnetic Properties of Ni-Ferrite Nanoparticles Synthesized by the Microwave-Combustion Method. *Ceramics International*, **41**, 11264-11271. <https://doi.org/10.1016/j.ceramint.2015.05.079>
- [15] Balavijayalakshmi, J., Suriyanarayanan, N. and Jayaprakash, R. (2015) Role of Copper on Structural, Magnetic and Dielectric Properties of Nickel Ferrite Nano Particles. *Journal of Magnetism and Magnetic Material*, **385**, 302-307. <https://doi.org/10.1016/j.jmmm.2015.03.036>
- [16] Doh, S.G., Kim, E.B., Lee, B.H. and Oh, J.H. (2004) Characteristics and Synthesis of Cu-Ni Ferrite Nanopowders by Coprecipitation Method with Ultrasound Irradiation. *Journal of Magnetism and Magnetic Material*, **272-276**, 2238-2240. <https://doi.org/10.1016/j.jmmm.2003.12.926>
- [17] Roumaïh, K. (2008) The Transport Properties of the Mixed Ni-Cu Ferrite. *Journal of Alloys and Compounds*, **465**, 291-295. <https://doi.org/10.1016/j.jallcom.2007.10.073>
- [18] Msomi, J. and Moyo, T. (2009) Effect of Domain Transformation on the Magnetic Properties of $Cu_xNi_{1-x}Fe_2O_4$ Ferrites. *Journal of Magnetism and Magnetic Material*, **321**, 1246-1250. <https://doi.org/10.1016/j.jmmm.2008.11.003>
- [19] Greiner, A. and Wendorff, J.H. (2007) Electrospinning: A Fascinating Method for

- the Preparation of Ultrathin Fibers. *Angewandte Chemie International Edition*, **46**, 5670-5703. <https://doi.org/10.1002/anie.200604646>
- [20] Lu, X.F., Wang, C. and Wei, Y. (2009) One-Dimensional Composite Nanomaterials: Synthesis by Electrospinning and Their Applications. *Small*, **21**, 2349-2370. <https://doi.org/10.1002/smll.200900445>
- [21] Safa, O.K. and Peter, C. (2006) Springer Handbook of Electronic and Photonic Materials. Springer-Verlag, New York, 349.
- [22] Xiang, J., Shen, X.Q., Song, F.Z. and Liu, M.Q. (2010) One-Dimensional NiCuZn Ferrite Nanostructures: Fabrication, Structure, and Magnetic Properties. *Journal of Solid State Chemistry*, **183**, 1239-1244. <https://doi.org/10.1016/j.jssc.2010.03.041>
- [23] Gabal, M.A., Al Angari, Y.M. and Kadi, M.W. (2011) Structural and Magnetic Properties of Nanocrystalline $Ni_{1-x}Cu_xFe_2O_4$ Prepared through Oxalates Precursors. *Polyhedron*, **30**, 1185-1190. <https://doi.org/10.1016/j.poly.2011.01.032>
- [24] Umare, S.S., Ningthoujam, R.S., Sharma, S.J., Shrivastava, S., Kurian, S. and Gajbhiye, N.S. (2008) Mossbauer and Magnetic Studies on Nanocrystalline $NiFe_2O_4$ Particles Prepared by Ethylene Glycol Route. *Hyperfine Interactions*, **184**, 235-243. <https://doi.org/10.1007/s10751-008-9796-4>
- [25] Rais, A., Taibi, K., Addou, A., Zanoun, A. and Al-Douri, Y. (2014) Copper Substitution Effect on the Structural Properties of Nickel Ferrites. *Ceramics International*, **40**, 14413-14419. <https://doi.org/10.1016/j.ceramint.2014.06.037>
- [26] Farghali, A.A., Khedr, M.H. and Abdel Khalek, A.A. (2007) Catalytic Decomposition of Carbon dioxide over Freshly Reduced Activated $CuFe_2O_4$ Nanocrystal. *Journal of Materials Processing Technology*, **181**, 81-87. <https://doi.org/10.1016/j.jmatprotec.2006.03.053>
- [27] Ponhan, W. and Maensiri, S. (2009) Fabrication and Magnetic Properties of Electrospun Copper Ferrite ($CuFe_2O_4$) Nanofibers. *Solid State Sciences*, **11**, 479-484. <https://doi.org/10.1016/j.solidstatesciences.2008.06.019>
- [28] Buschow, K.H.J. (1995) Handbook of Magnetic Materials. Vol. 8, North-Holland, Amsterdam, 212.